

Bifurcation and chaotic behavior in the Euler method for a Uçar prototype delay model

Mingshu Peng

Department of Mathematics, Beijing Jiao Tong University, Beijing 100 044, People's Republic of China

Accepted 24 February 2004

Abstract

A discrete model with a simple cubic nonlinearity term for the symmetric coupling of three fixed points (one unstable) is treated in the study of bifurcations and chaotic behavior of a prototype delayed dynamical system under discretization. Effective computation of Hopf bifurcations, stable limit cycles (periodic solutions), symmetrical breaking bifurcations and chaotic behavior in nonlinear delayed equations is proposed.

© 2004 Elsevier Ltd. All rights reserved.

1. Introduction

In [18,19], a prototyped delay model with cubic nonlinearity

$$\dot{x}(t) = \delta x(t - \tau) - \epsilon [x(t - \tau)]^3$$

or equivalently (by changing the scale by $t' = \tau t$)

$$\dot{x}(t) = \delta \tau x(t - 1) - \epsilon \tau [x(t - 1)]^3 \quad (1.1)$$

has been proposed and its complex dynamical behavior has been studied in detail by the use of fifth order Runge–Kutta ordinary differential solver embedded in Matlab toolbox [17] for 0.01 integration step-size and 10^{-6} absolute and relative tolerance, where δ and ϵ are positive parameters and τ is delay time.

It is easily simulated by numerical computation at least qualitatively and observed that the limit set of numerical solutions changes from a stable equilibrium point into an invariant closed curve, invariants loops and eventually chaotic behavior by varying the parameter value. As to the study of Hopf bifurcation and periodic solutions in numerical approximation of delay differential equations, see [3–5,10,11] by use of the Euler method and [7] by Runge–Kutta discretization.

In this note, we propose a discrete model by Euler method (a simple yet efficient way) to explore the rich dynamics of delay differential equations, and present an implementation of the methods and our numerical experience. The main results come from the estimate of the Large Lyapunov exponent and the amplitude of the trivial attractor (fixed points or limit cycles) or strange attractor.

Employing the techniques and methods developed in this paper, complex dynamical behavior of delay differential equations can be explored clearly, e.g., we obtain similar results to Uçar [18,19] and Strogatz [16] (see Section 4).

This paper is organized as follows: In Section 2, a discrete model has been defined. Some properties for Eqs. (2.1) and (2.2) have been discussed in Section 3. The global behavior of the model has been delved into in Section 4, where a

E-mail address: mshpeng@center.njtu.edu.cn (M. Peng).

bifurcation diagram is provided to observe the effect of time delay, and a phenomenon of multiple bifurcations is also observed. Finally, in Section 5 the findings are summarized and conclusions are drawn.

2. The discrete model

For simplicity of analysis, we consider step-sizes of the form $h = 1/n$, where n is a positive integer. The Euler method applied to (1.1) yields the delay difference equation (DDE)

$$u(k + 1) = u(k) + \alpha(\delta, \tau, n)u(k - n) - \beta(\epsilon, \tau, n)u(k - n)^3, \tag{2.1}$$

where $\alpha(\delta, \tau, n) = \delta\tau/n$, $\beta(\epsilon, \tau, n) = \epsilon\tau/n$, $u(k)$ is an approximate value to $x(kh)$. As to the study of Neimark–Saker bifurcation and chaotic behavior of (2.1) for $\delta = \epsilon < 0$, see [11]. And for the study of Hopf bifurcation and periodic solutions of (1.1) with $\delta = \epsilon < 0$, see [1,2] and the references therein. If given $n + 1$ arbitrary real valued numbers $a(k_0 - n), a(k_0 - n + 1), \dots, a(k_0)$, Eq. (2.1) has a unique solution $\{u(k)\}_{k_0-n}^{\infty}$ satisfying the initial condition

$$u(k) = a(k) \text{ for } k \in [k_0 - n, k_0]. \tag{2.2}$$

In this paper the following notation is used throughout. \mathbb{R}^n denotes the n -dimensional Euclidean space and $\det A$ is determinant of a matrix A . σ_1 denotes the largest Lyapunov exponent of system (2.1). α_n denotes $\alpha(\delta, \tau, n)$, β_n denotes $\beta(\epsilon, \tau, n)$.

3. Some properties

By introducing new variables $x_{i+1}(k) = u(k - i)$ ($i = 0, 1, \dots, n$), we can rewrite (2.1) in the following form:

$$x(k + 1) = \begin{pmatrix} x_1(k + 1) \\ x_i(k + 1) \end{pmatrix} = F(x(k)) = \begin{pmatrix} x_1(k) + \alpha(\delta, \tau, n)x_{n+1}(k) - \beta(\epsilon, \tau, n)x_{n+1}(k)^3 \\ x_{i-1}(k) \end{pmatrix}, \tag{3.1}$$

where $i = 2, \dots, n + 1$, $\alpha(\delta, \tau, n) > 0$, $\beta(\epsilon, \tau, n) > 0$ and $x \in \mathbb{R}^{n+1}$. They consist of a n -dimensional linear subsystem and an one-dimensional nonlinear subsystem. Thus, only in one of the $n + 1$ -dimensional nonlinear folding and stretching occurs in one of the variables (x_n). In all the other variables a simple mapping from x_{i-1} onto x_i take place. So mappings (3.1) can be viewed as one of the simplest systems capable of showing higher-dimensional chaos.

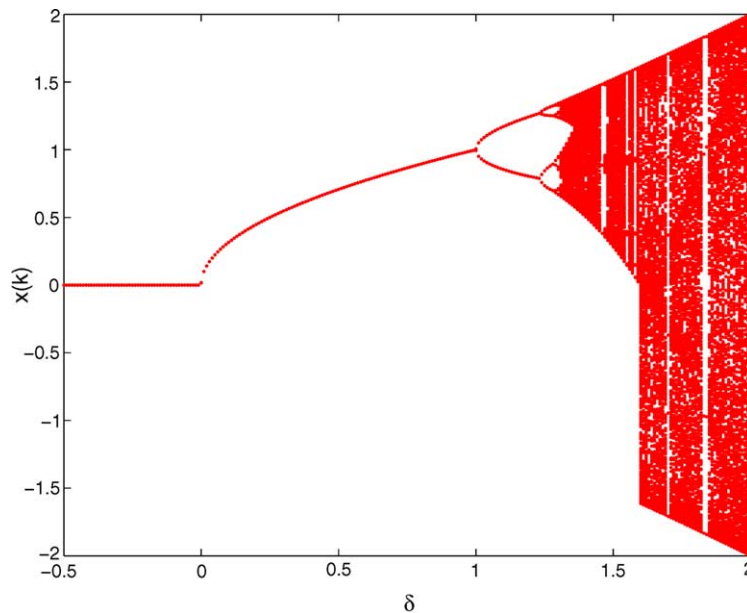


Fig. 1. Bifurcation diagram of the 1D-Map: $-0.5 \leq \delta \leq 2$ for $\epsilon = 1$.

Consider the fixed points \bar{x} of system (2.1) and their stability. From $F(\bar{x}) = \bar{x}$, we obtain

$$\bar{x}_0 = \overbrace{(0, 0, \dots, 0)^T}^{n+1 \text{ times}}$$

and other two fixed points for system (3.1) are

$$\bar{x}_{\pm} = \underbrace{(\pm\sqrt{\delta/\epsilon}, \pm\sqrt{\delta/\epsilon}, \dots, \pm\sqrt{\delta/\epsilon})^T}_{n+1 \text{ times}}.$$

The stability of the fixed points \bar{x}_{\pm} is governed by the eigenvalues of the Jacobian of the map (3.1).

Obviously,

$$A = \left. \frac{\partial F}{\partial x} \right|_{x=\bar{x}_{\pm}} = \begin{pmatrix} 1 & 0 & \dots & 0 & \alpha_n - 3\delta\beta_n/\epsilon \\ 1 & 0 & \dots & 0 & 0 \\ \vdots & \vdots & & \vdots & \vdots \\ 0 & 0 & \dots & 1 & 0 \end{pmatrix}. \tag{3.2}$$

Note that $\det A = (-1)^{(n)}(\alpha_n - 3\delta\beta_n/\epsilon)$ and $\alpha_n - 3\delta\beta_n/\epsilon = -2\delta\tau/n$, one can get the system is dissipative [6,15] for $|\delta\tau| < n/2$.

The characteristic polynomial of A is

$$Q(\lambda) = \det(\lambda I - A) = \lambda^{n+1} - \lambda^n + 2\delta\tau/n = 0. \tag{3.3}$$

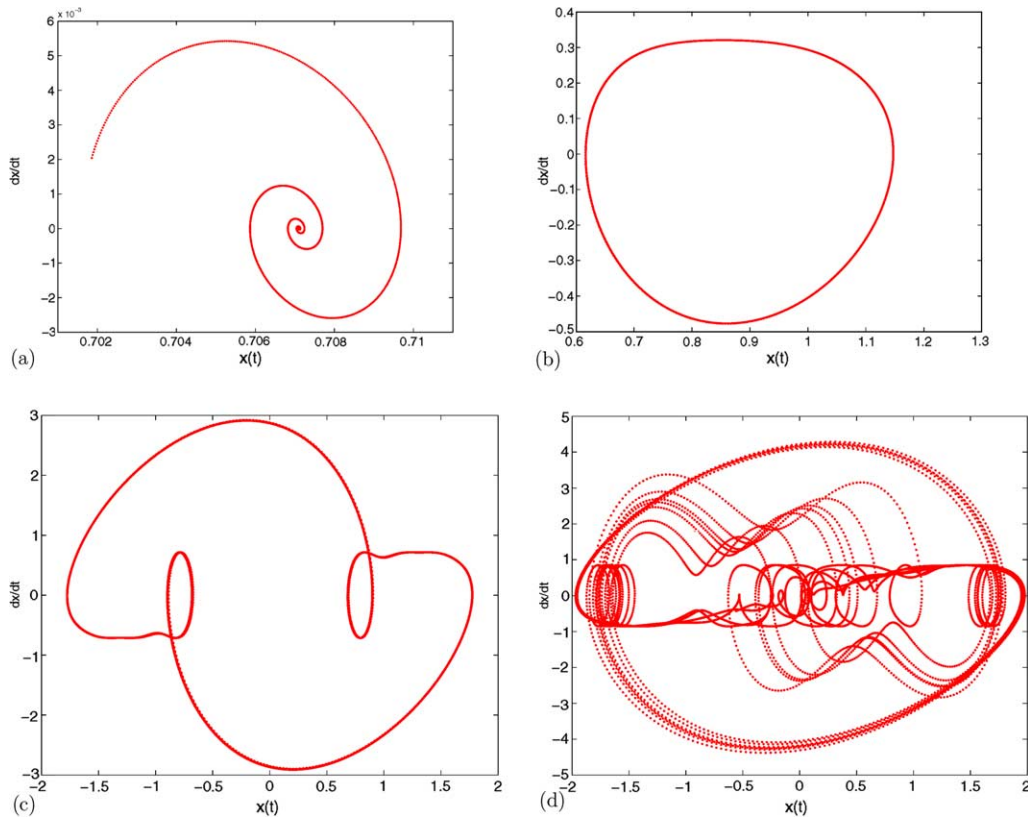


Fig. 2. Phase portrait of Eq. (1.1) (also system (4.2)) with $\tau = \epsilon = 1$: (a) for $\delta = 0.5$ system trajectory converges to the equilibrium point; (b) self-sustained oscillation for $\delta = 0.9$; (c) oscillation for $\delta = 1.51$; (d) chaotic behavior for $\delta = 1.7$. First hundreds of points are not plotted. (See Fig. 4 [19] by the use of fifth order Runge–Kutta ordinary differential solver embedded in Matlab toolbox [17] for 0.001 integration step-size and 10^{-6} absolute and relative tolerance.)

A fixed point is locally asymptotically stable if all the roots of the characteristic polynomial have modulus less than one. It is shown by Levin and May [13] (also see [12]) that the absolute values of all the roots of (3.3) are less than one if and only if $0 < 2\delta\tau/n < 2\cos[n\pi/(2n + 1)]$, i.e.,

$$0 < \delta\tau < \gamma_n^* \triangleq n \cos[n\pi/(2n + 1)]. \tag{3.4}$$

This γ_n^* is a prospective value at which a Neimark–Sacker (Hopf) bifurcation occur (see, e.g. [8,10,11,20]).

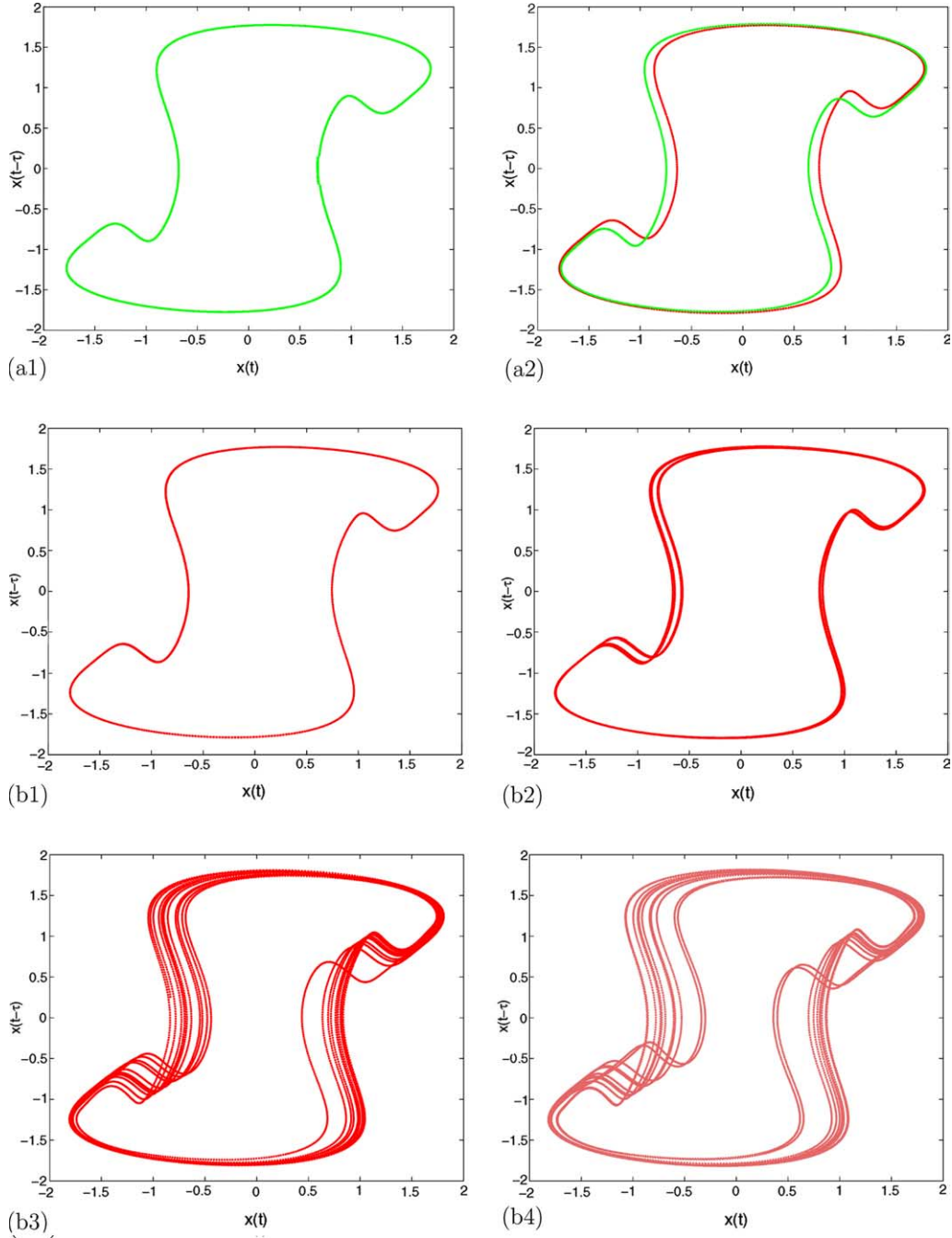


Fig. 3. Multiple limit cycle bifurcations of Eq. (1.1) (approximated by system (4.2)) with $\tau = \epsilon = 1$ for $1.51 \leq \delta \leq 1.55$: (a1–a2) symmetry breaking bifurcation for $\delta = 1.51$ and 1.52 ; (b1–b4) period-doubling bifurcations for $\delta = 1.52, 1.53, 1.54,$ and 1.55 respectively.

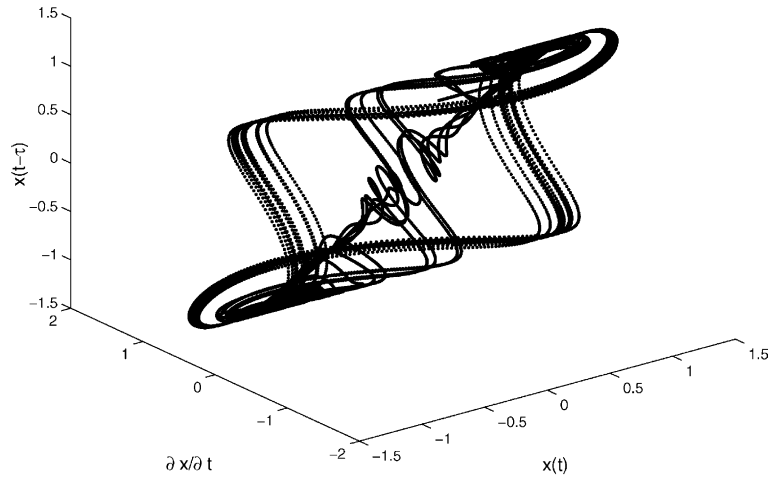


Fig. 4. A typical trajectory of the model (1.1) (approximated by system (4.2)) for $\epsilon = \delta = 1$ and $\tau = 1.65$ (see Fig. 4 [18]).

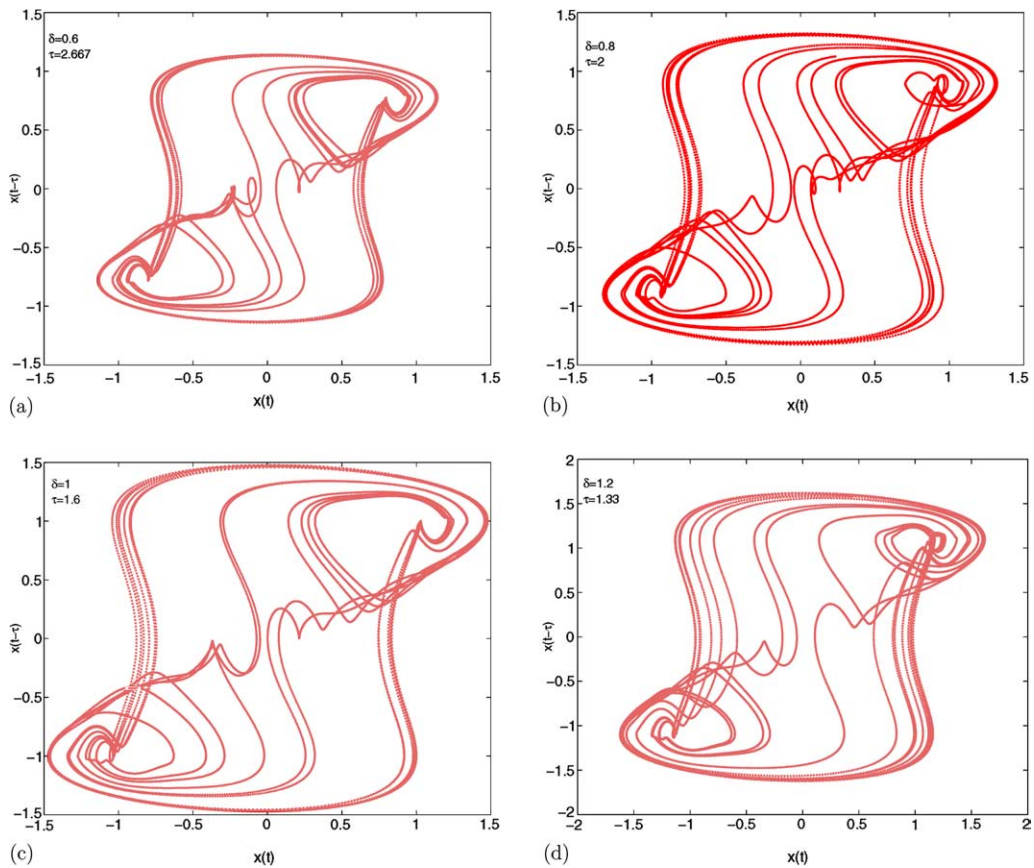


Fig. 5. Chaotic behavior of $\delta\tau = 1.6$ mode for model (1.1) (approximated by system (4.2)) with the same greatest Lyapunov exponent $\sigma = 0.0016$ (20,000 iterations, $N_0 = 256$ different initial states set on the chaotic attractor; the last half part of iterations are plotted as above): (a) for $\delta = 0.6$, $\tau = 2.667$; (b) for $\delta = 0.8$, $\tau = 2$; (c) for $\delta = 1$, $\tau = 1.6$; (d) for $\delta = 1.2$, $\tau = 1.33$. (a) $\delta = 8.55$, $\tau = 0.2$; (b) $\delta = 1.71$, $\tau = 1$; (c) $\delta = 1$, $\tau = 1.71$; (d) $\delta = 0.171$, $\tau = 10$ (see Fig. 9 [18]).

As to the trivial fixed point \bar{x}_0 , one can obtain the Jacobian matrix as follows:

$$B = \frac{\partial F}{\partial x} \Big|_{x=\bar{x}_0} = \begin{pmatrix} 1 & 0 & \dots & 0 & \alpha_n \\ 1 & 0 & \dots & 0 & 0 \\ \vdots & \vdots & & \vdots & \vdots \\ 0 & 0 & \dots & 1 & 0 \end{pmatrix}. \tag{3.5}$$

The characteristic polynomial of B is

$$Q(\lambda) = \det(\lambda I - B) = \lambda^{n+1} - \lambda^n - \alpha_n = 0. \tag{3.6}$$

Therefore, according to Levin and May [13] and Kuruklis [12], the fixed point \bar{x}_0 is unstable because of $\alpha_n > 0$.

4. Numerical results

Let us now turn to numerical investigations for $n = 0$ (without delay) and $n = 100$ with initial value conditions $x_i(0) = 0.1, i = 1, 2, \dots, n + 1$ and $\Phi(t) = 0.1, -\tau \leq t \leq 0$ for system (1.1).

As to the case $n = 0$, i.e., $\tau = 0$ in system (1.1) and the Euler method is applied to system (1.1) with step-size $h = 1$ and $\dot{x}(k) \approx x(k + 1) - x(k)$, we give a brief study of the 1D-map

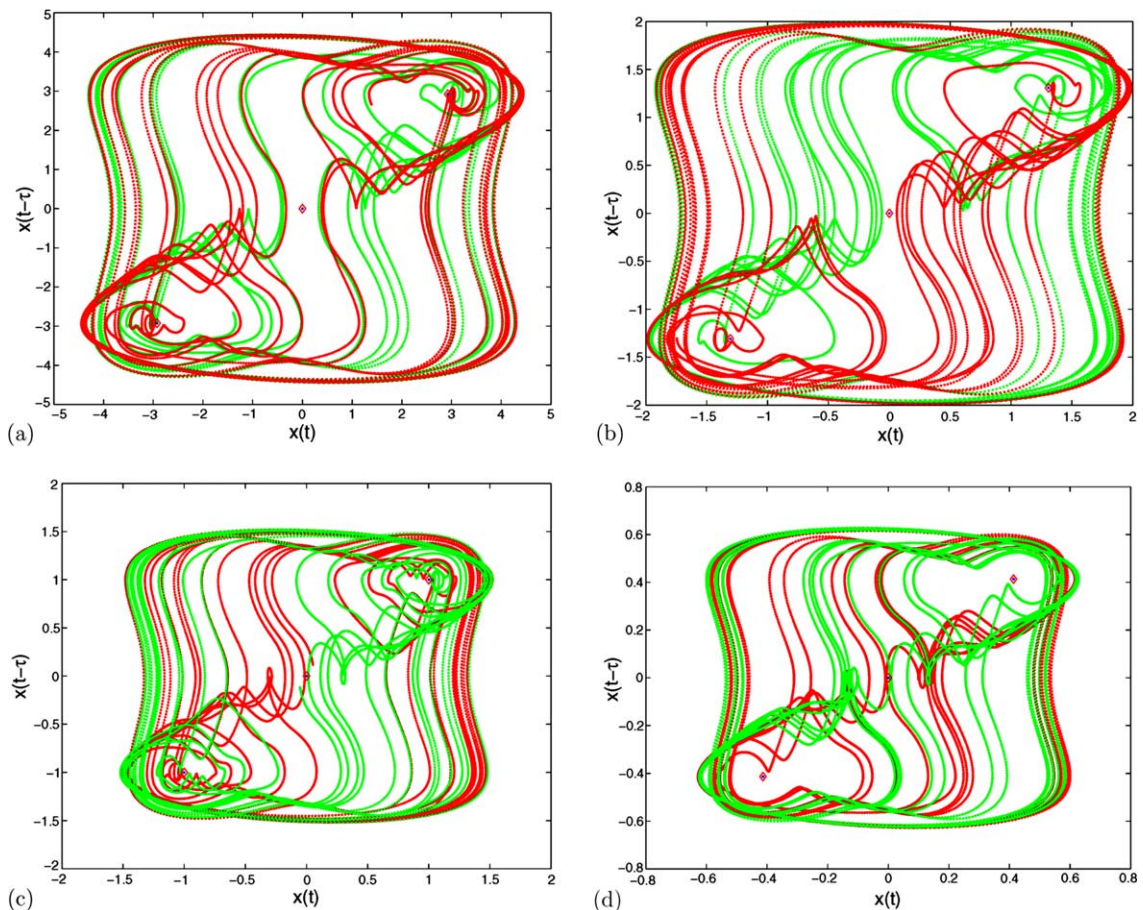


Fig. 6. Chaotic behavior of $\delta\tau = 1.71$ mode for model (1.1) (approximated by system (4.2)) with the same greatest Lyapunov exponent $\sigma = 0.0033$ (30,000 iterations, $N_0 = 256$ different initial states set on the chaotic attractor; the last 10,000 of the iterations are plotted as above). (a) $\delta = 8.55, \tau = 0.2$; (b) $\delta = 1.71, \tau = 1$; (c) $\delta = 1, \tau = 1.71$; (d) $\delta = 0.171, \tau = 10$.

$$x(k + 1) = x(k)(1 + \delta - \epsilon x(k)^2). \tag{4.1}$$

As the parameters of nonlinear system (4.1) change, the stability of the equilibriums changes as well as the number of equilibrium points. If the parameter δ passes through zero from negative to positive, the trivial stable fixed point splits into three points. Dynamically, a symmetry-breaking pitchfork bifurcation occurs; one center (attractor) is transformed into a unstable saddle point at the origin (repellor) and two centers (attractors) located at $\pm\sqrt{\delta/\epsilon}$, which coincides exactly with the results shown in [16,18]. Subsequently, period-doubling bifurcations occur and higher-periodic orbits

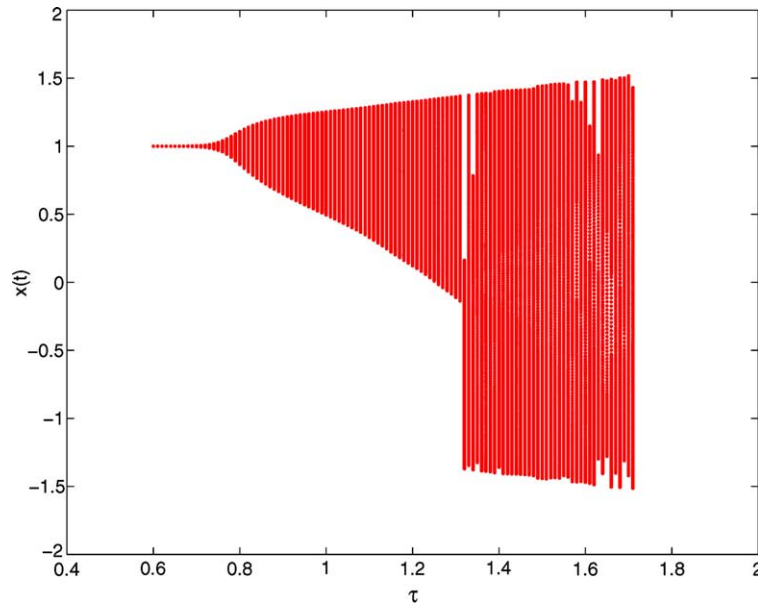


Fig. 7. Bifurcation diagram of model (1.1) (approximated by system (4.2)) for a range of time delay $\tau : 0.6 \leq \tau \leq 1.72$ for $\delta = \epsilon = 1$.

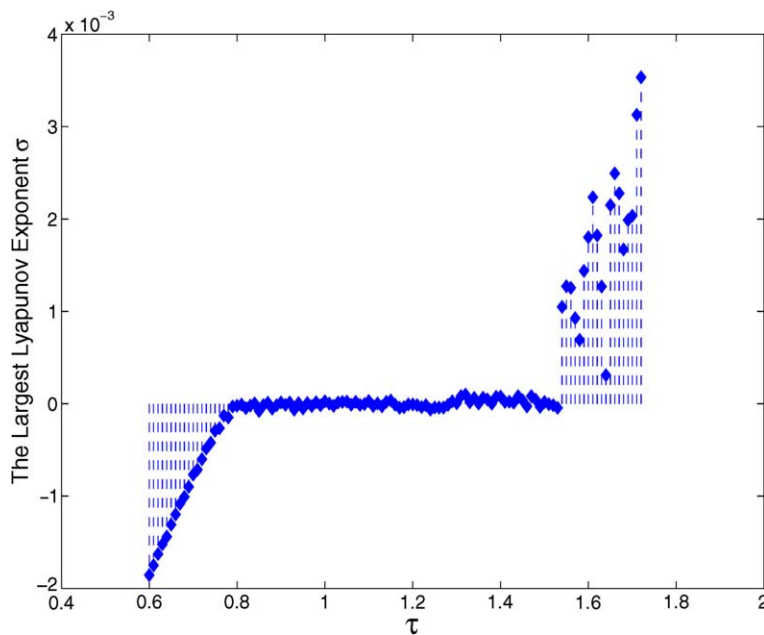


Fig. 8. The largest Lyapunov exponent σ of model (1.1) (approximated by system (4.2)) for $0.6 \leq \tau \leq 1.72$.

become stable until two local chaotic regions sets in; after the symmetry-increasing crisis [14], these two regions cross together and there exists a global chaotic region. The bifurcation diagram in Fig. 1 gives a graphic description of this scenario for $\epsilon = 1$.

Now, we consider the 101D-map

$$x(k+1) = \begin{pmatrix} x_1(k) + 0.01\delta\tau x_{101}(k) - 0.01\epsilon\tau x_{101}(k)^3 \\ x_1(k) \\ \vdots \\ x_{100}(k) \end{pmatrix}, \tag{4.2}$$

where $x \in \mathbb{R}^{101}$, i.e., the Euler method is applied to (1.1) with step-size $h = 0.01\tau$, $t = kh$, $x(t - \tau) = x(kh - \tau) \approx u(k - 100) = x_{101}(k)$, $x(t) \approx x_1(k)$ and $\dot{x}(t) \approx (x(kh + h) - x(kh))/h \approx (x_1(k + 1) - x_1(k))/h$. Computer simulation with 10^{-4} absolute and relative tolerance shows that numerical results similar to those proposed in [18,19] can be obtained, see Figs. 2–6 and 9.

Using the method employed in this paper, a different bifurcation diagram (see Figs. 7 and 8) from [18] is presented to delve into the detail effects of the time delay on the model behaviors for fixed model parameters of $\delta = \epsilon = 1$. Fig. 7 shows a one-parameter bifurcation diagram changing delay time τ along the interval $[0.6, 1.72]$. The results presented in Fig. 7 are obtained such that the model response for chosen set of the parameters were monitored for $[0, 6000]$ simulation time with $x_0 = 0.5$ and their last thousand parts are considered to present state dynamic.

Figs. 7 and 8 show the model output, x first converges to the stable fixed point $x = 1$ for $0.6 \leq \tau \leq 0.78^{\pm}(100 \cos(100\pi/201))$ for model (4.2) or $\pi/4$ for system (1.1) then to a stable invariant closed limit cycle (periodic

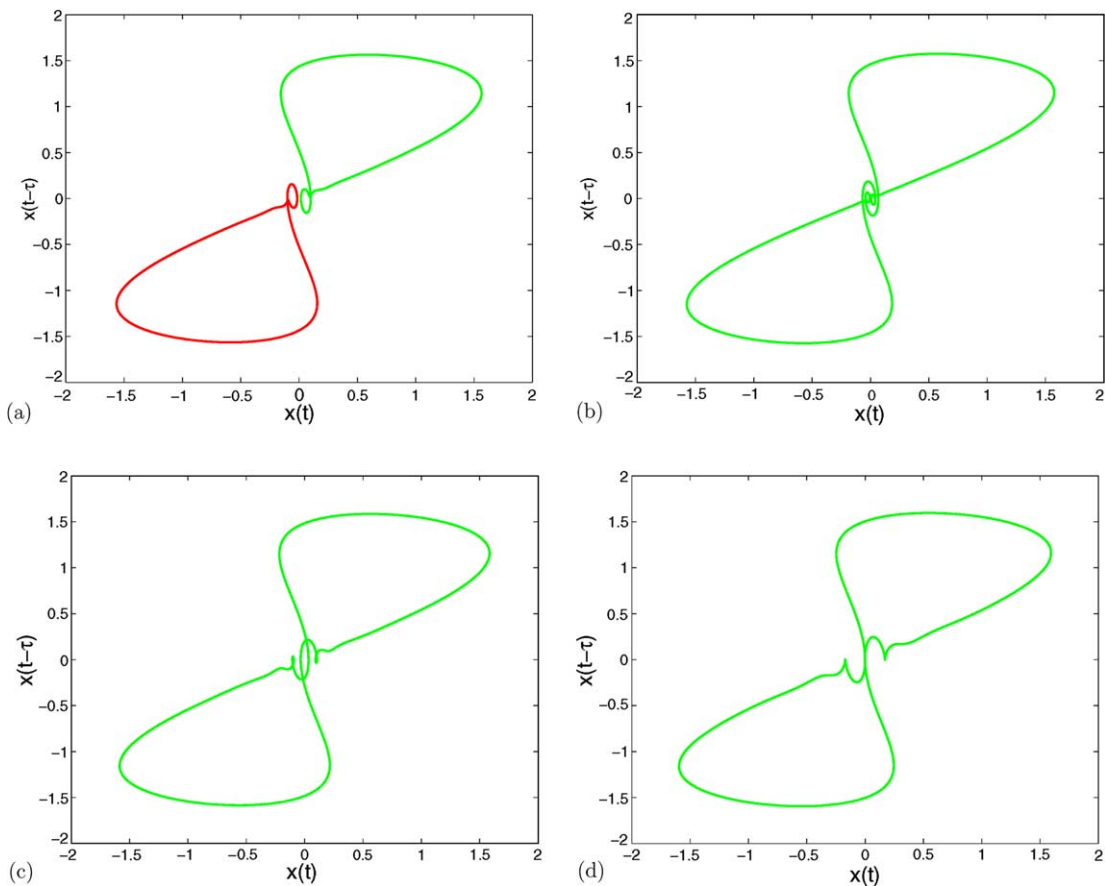


Fig. 9. Trajectories of system (1.1) (approximated by model (4.2)) with $\delta = \epsilon = 1$ with increasing symmetry and multiple limit cycle bifurcations as the parameter τ changes: (a) $\tau = 1.31$, two unconnected limit cycles; (b–d) connected limit cycles with special symmetry $x(\cdot + a) = -x$ for (b) $\tau = 1.32$, (c) 1.33 and (d) 1.34 respectively.

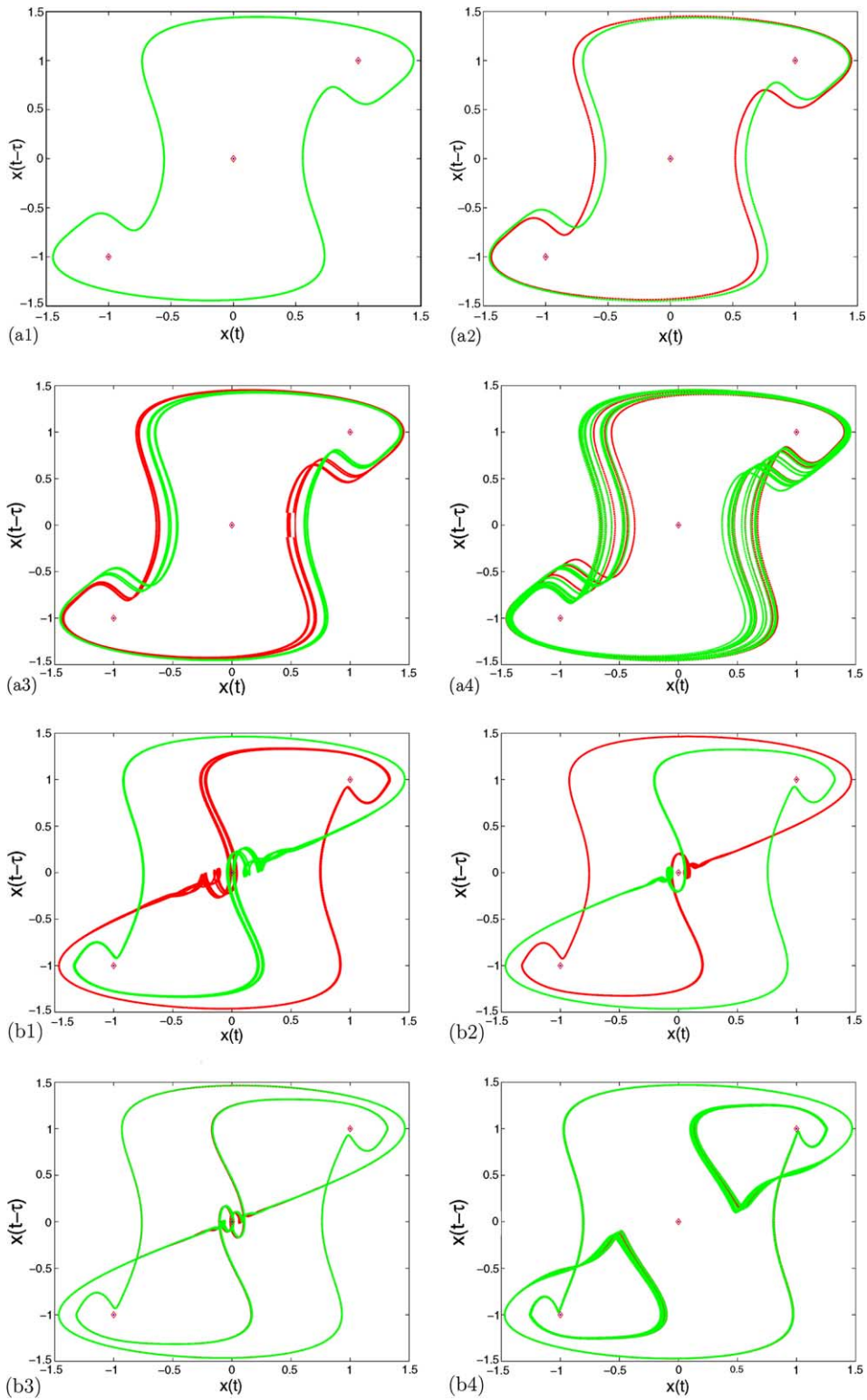


Fig. 10. Multiple bifurcations of system (1.1) (approximated by system (4.2)) with $\delta = \epsilon = 1$ with initial functions $\Phi(t) = \pm 0.1$. (a1) $\tau = 1.51$, (a2) $\tau = 1.52$, (a3) $\tau = 1.53$, (a4) $\tau = 1.54$, (b1) $\tau = 1.574$, (b2) $\tau = 1.576$, (b3) $\tau = 1.578$, (b4) $\tau = 1.58$, (c1) $\tau = 1.641$, (c2) $\tau = 1.643$ (see Fig. 7 [18]).

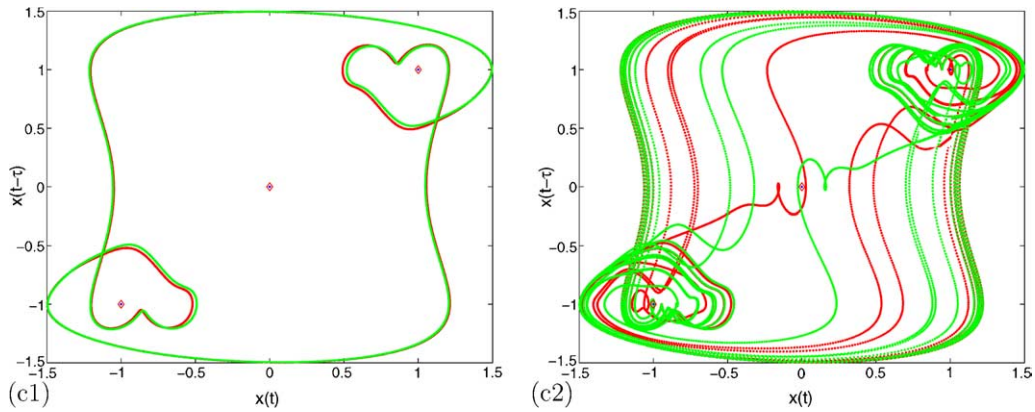


Fig. 10 (continued)

Table 1
A comparison between our results for system (1.1) and those by [18]

Content	Uçar's results	Our results
Numerical method	Runge–Kutta method	Euler method
Initial function $\phi(t)$	$\phi(t) = 0.1$	$\phi(t) = 0.1$
Step-size h	$h = 0.01$	$h = 0.01$
The first chaotic region ($\epsilon = \tau = 1$)	$\delta \approx 1.56$	$\delta \approx 1.54$
The first chaotic region ($\delta = \epsilon = 1$)	$\tau \approx 1.55$	$\delta \approx 1.54$
The second chaotic region ($\delta = \epsilon = 1$)	–	$\tau \approx 1.58$
The third chaotic region ($\delta = \epsilon = 1$)	$\tau \approx 1.64$	$\tau \approx 1.641$
Unbounded response ($\epsilon = \tau = 1$)	$\delta \geq 1.8$	$\delta \geq 1.72$
Unbounded response ($\delta = \epsilon = 1$)	$\tau \approx 1.75$	$\tau \approx 1.73$

solution). After the symmetry-increasing crisis, the first chaotic region sets about at $\tau \approx 1.54$ (Figs. 9 and 10(a1)–(a4)). Further increasing τ leads to a multiple bifurcation again and then the second chaotic region (Fig. 10(b1)–(b4)) and then the third chaotic region (Figs. 5 (c) and 10(c1)–(c2)). The model exhibits unbounded response for $\tau \geq 1.73$.

Now, we end this section with Table 1 which shows a comparison between our results for system (1.1) and those by Uçar [18].

5. Conclusions

In this paper, we study the bifurcation and chaotic behavior in a class of delay difference equations (DDE). Analytical and numerical results for maps of lower and higher dimensions have been collected. Computer simulations show that similar results to a prototype delay dynamical system can be obtained, such as the stability of the fixed point, the occurrence of stable quasi-periodic solutions, invariant loops, and eventually chaotic dynamical behavior.

By considering the DDE, chaotic behavior of nonlinear delay-differential systems (DDS) can be studied, although the delay system here only contains a single cubic term depending on one variable as nonlinearity. A method of using a finite-dimensional discrete dynamical system to approximate an infinite-dimensional dynamical system is developed here. This also illustrate that many results in the theory of difference equations has been obtained as much or less natural discrete analog of corresponding results of differential equations [9]. So, the DDE gives a family of examples for chaotic behavior usable to demonstrate analyzing and controlling schemes.

Acknowledgements

Research partially supported by NSFC, Tianyuan Foundation (A0324622) and Research Foundation of Beijing Jiao Tong University.

References

- [1] Dormayer P. The stability of special symmetric solutions of with small amplitudes. *Nonlinear Anal TMA* 1990;14(8):701–15.
- [2] Faria T, Magalhães LT. Normal forms for retarded functional differential equations with parameters and applications to Hopf bifurcation. *J Diff Eqs* 1995;122:181–200.
- [3] Ford NJ, Wulf V. The use of boundary locus plots in the identification of bifurcation points in numerical approximation of delay differential equations. *J Comput Appl Math* 1999;111:153–62.
- [4] Haderer KP. Effective computation of periodic orbits and bifurcation diagrams in delay equations. *Numer Math* 1980;34:457–67.
- [5] Hairer E, Norsett SP, Wanner G. Solving ordinary differential equations I. Springer series in computational mathematics, vol. 8. Berlin: Springer; 1987.
- [6] Hao BL. Elementary symbolic dynamics and chaos in dissipative systems. Singapore: World Scientific; 1989.
- [7] Hout K In't, Lubich C. Periodic orbits of delay differential equations under discretization. *BIT* 1998;38(1):72–91.
- [8] Iooss G. Bifurcation of maps and applications. Amsterdam: North-Holland; 1979.
- [9] Kaymakçalan B, Lakshmikantham V, Sivasundaram S. Dynamical systems on measure chain. Dordrecht: Kluwer-Academic; 1996.
- [10] Koto T. Neimark–Sacker bifurcations in the Euler method for a delay differential equation. *BIT* 1998;39(1):110–5.
- [11] Koto T. Periodic orbits in the Euler methods for a class of delay differential equations. *Comput Math Appl* 2001;42:1597–608.
- [12] Kuruklis SA. The asymptotic stability of $x_{n+1} - ax_n + bx_{n-k} = 0$. *J Math Anal Appl* 1994;188:719–31.
- [13] Levin SA, May RM. A note on difference–delay equations. *Theoret Popul Biol* 1976;9:178–87.
- [14] Melbourne I, Dellnitz M, Golubitsky M. The structure of symmetric attractors. *Arch Ration Mech Anal* 1993;123:75–98.
- [15] Richter H. The generalized Henon maps: examples for higher-dimensional chaos. *Int J Bifurc Chaos* 2002;12(6):1371–84.
- [16] Strogatz SH. In: *Nonlinear dynamics and chaos: with application to physics, biology, chemistry and engineering*, vol. 16. Massachusetts: Addison-Wesley Publishing Company; 1994. pp. 187–194.
- [17] The MathWork Inc. Matlab Version 5.1. Natic: MathWorks Inc, MA, 1997.
- [18] Uçar A. On the chaotic behavior of a prototype delayed dynamical system. *Chaos, Solitons & Fractals* 2003;16:187–94.
- [19] Uçar A. A prototype model for chaos studies. *Int J Eng Sci* 2002;40:251–8.
- [20] Wiggins S. Introduction to applied nonlinear dynamical systems and chaos. Berlin: Springer-Verlag; 1990.